

Analysis of electrochemical double-layer capacitors using a Natural Rubber-Zn based polymer electrolyte

Nanditha Rajapaksha^a, Kumudu S. Perera^{*} and Kamal P. Vidanapathirana^b

Polymer Electronics Research Group, Department of Electronics, Wayamba University of Sri Lanka, Kuliyaipitiya, Sri Lanka

(Received June 10, 2021, Revised November 5, 2021, Accepted November 20, 2021)

Abstract. Electrochemical double-layer capacitors (EDLCs) based on solid polymer electrolytes (SPEs) have gained an immense recognition in the present world due to their unique properties. This study is about preparing and characterizing EDLCs using a natural rubber (NR) based SPE with natural graphite (NG) electrodes. NR electrolyte was consisted with 49% methyl grafted natural rubber (MG49) and zinc trifluoromethanesulfonate ((Zn(CF₃SO₃)₂-ZnTF). It was characterized using electrochemical impedance spectroscopy (EIS) test, dc polarization test and linear sweep voltammetry (LSV) test. NG electrodes were made using a slurry of NG and acetone. EIS test, cyclic voltammetry (CV) test and galvanostatic charge discharge (GCD) test have been done to characterize the EDLC. Optimized electrolyte composition with NR: 0.6 ZnTF (weight basis) exhibited a conductivity of $0.6 \times 10^{-4} \text{ Scm}^{-1}$ at room temperature. Conductivity was predominantly due to ions. The electrochemical stability window was found to be from 0.25 V to 2.500 V. Electrolyte was sandwiched between two identical NG electrodes to fabricate an EDLC. Single electrode specific capacitance was about 2.26 Fg^{-1} whereas the single electrode discharge capacitance was about 1.17 Fg^{-1} . The EDLC with this novel NR-ZnTF based SPE evidences its suitability to be used for different applications with further improvement.

Keywords: electrochemical double-layer capacitors; natural graphite; natural rubber; single electrode specific capacitance; solid polymer electrolytes

1. Introduction

Electrochemical double layer capacitor (EDLC)s belong to the family of energy storage devices and they can store relatively higher energy density than that of conventional capacitor. Their key advantages include fast charging/discharging (high power density), long charge-discharge cycles, broad operating temperature ranges etc. They have found wide applications in hybrid and electric vehicles, electronics, aircrafts, and smart grids etc. (Libich *et al.* 2018, Abruña *et al.* 2008). They can be fabricated using two identical electrodes (known as ‘symmetric EDLCs’) as well as two different types of electrodes (known as ‘asymmetric EDLCs’). A typical symmetric EDLC is composed of a suitable electrolyte with two carbon based electrodes (Yu *et al.* 2012). Often the

^{*}Corresponding author, Professor, E-mail: kumudu31966@gmail.com

^aPh.D. Student, E-mail: nanditharajapaksha2@gmail.com

^bProfessor, E-mail: kamalpv41965@gmail.com

electrolyte has been an aqueous or non-aqueous liquid electrolyte. However, challenges of practically handling a liquid electrolyte in an EDLC, have led to search for solid electrolytes with promising features.

Solid polymer electrolytes (SPEs) are one such solid electrolyte category employed for batteries, fuel cells, sensors and electrochromic displays (Simon *et al.* 2008, Nimah *et al.* 2015, Pal and Ghosh 2018). Polymers such as poly(ethylene oxide) (PEO), poly vinylidene fluoride (PVdF) and poly vinylidene fluoride co hexafluoropropylene (PVdF-Co-HFP) have been used in SPE formulations.

A good conductivity, stability, environmental compatibility (eg. low toxicity, natural abundance) and affordability are key desirable properties of successful electrolytes. However, the typical conductivity of most SPEs is still in the order of 10^{-5} Scm^{-1} which is significantly lower than that of desired conductivity range (e.g., 10^{-3} - 10^{-4} Scm^{-1}) and hence, various methodologies have been launched to improve conductivity of SPEs. One method is replacing PEO with other suitable polymers. Salleh *et al.* have reported about a study on a SPE based on methyl cellulose biopolymer in place of PEO (Salleh *et al.* 2016). Having ammonium iodide as the salt, it had exhibited a conductivity of 5.08×10^{-4} Scm^{-1} . Another approach to improve the conductivity of SPEs is blending several polymers to get use of characteristics of each polymer. Chandra, A. has synthesized a poly(ethylene oxide) and poly(vinylpyrrolidone) blended SPE with a good conductivity (Chandra 2013). Nevertheless, there are some detriments in commercial polymers, such as toxicity, environmental impacts and high cost. To avoid these facts, natural polymers have been emerged as a prospective class of alternatives.

It is in this context that the choice of natural rubber (NR) as a polymeric media for SPE becomes attractive (Aziz *et al.* 2018). NR is obtained as a milky white fluid known as latex from the tropical rubber tree (*hevea brasiliensis*). Monomer of NR is isoprene (2-methyl-1,3-butadiene) which is a conjugated diene hydrocarbon. Most of the double bonds in the NR polymer chain give rise to natural rubber's elastomer qualities. As NR is an electric insulator, suitable modifications are required for the polymer chain to make it conducting up to the desired level to be able to use for a SPE in a diverse range of applications (Glasse *et al.* 2002, Idris *et al.* 2001, Silakul and Margaraphan 2013). Modified natural rubber (MNR) has a low glass transition temperature (T_g), soft elastomer characteristics at room temperature, good elasticity and possess adhesive properties which favor device fabrication.

One of the widely used modifications is the graft polymerization with methylmethacrylate (MMA) monomer (Idris *et al.* 2001). According to the number of monomers grafted to the NR polymer chain, such methyl grafted NR samples are named. As an example, if the number of MMA monomers incorporated to NR polymer chain is 49, it is labeled as MG49 (MG means methyl grafted). Such MG NR bears the combined properties of polymethylmethacrylate (PMMA) as well as NR. Provision of ion conduction is assumed to be due to PMMA whereas NR is responsible for elastic properties (Mohamed *et al.* 2008).

This paper is intended to report the preparation, optimization and characterization of a SPE based on MGNR and its performance in an electrochemical double layer capacitor (EDLC) having two identical graphite electrodes. The reporting SPE consists with MG49 NR and zinc trifluoromethanesulfonate ($(\text{Zn}(\text{CF}_3\text{SO}_3)_2\text{-ZnTF})$). Compositions of SPEs were optimized to get the highest conductivity. Investigations were carried out to identify conduction mechanism, mobility of charge species and electrochemical stability. EDLCs were fabricated using the SPE with the optimized composition and two identical natural graphite (NG) electrodes. They have been investigated using electrochemical impedance spectroscopy (EIS), cyclic voltammetry (CV) and galvanostatic charge-discharge (GCD) tests.

2. Materials and methods

2.1 Materials

MG49 NR was received from Associated Speciality Rubber (PVT) Ltd in Kegalle, Sri Lanka and zinc trifluoromethanesulfonate ($\text{Zn}(\text{CF}_3\text{SO}_3)_2\text{-ZnTf}$, 98%) was purchased from Sigma-Aldrich. Tetrahydrofuran (THF) purchased from Sigma-Aldrich was used as the solvent in the SPE. Well-cleaned fluorine-doped tin oxide (FTO) glass plates (Sigma-Aldrich) were used for the fabrication of EDLC. Natural graphite (NG) which was received from Bogala Graphite Lanka Ltd., Bogala, Sri Lanka was used without any prior treatment. Acetone (Sigma- Aldrich) was used as the solvent for preparing electrodes.

2.2 Preparation of SPEs

Selected amount of MG49 sample was minced into smaller pieces and mixed in THF. It was kept for 24 hours without stirring and then magnetic stirring was done for 24 hours. ZnTF solution was prepared separately in THF and stirred well. The two solutions of MG49 and ZnTF were then mixed together and stirred further to form a homogenous electrolyte solution. The final solution was then poured into a petri dish and left to slowly evaporate the solvent for 24 hours. Thereby, a thin electrolyte film could be obtained. SPEs having different salt concentrations were prepared keeping the amount of NR constant.

2.3 AC conductivity measurements of SPEs

AC conductivity measurements of a sample are connected with impedance data gathered throughout a range of frequencies. Using impedance data, conductivity can be calculated for different sample compositions at different temperatures. A circular shape sample was cut from the electrolyte film and it was assembled in between two stainless steel (SS) electrodes in a spring-loaded sample holder. Impedance data were gathered in the frequency range from 0.1 Hz to 400 kHz by using a computer controlled Metrohm Autolab Impedance Analyzer M101 from room temperature to 55°C. Thickness of the films was measured using a micrometer screw gauge.

2.4 Transference number measurements

Transference number measurements are recognized as finger prints for the contribution of different charge species on the conductivity. In the present study, it was evaluated by the mobility of each charge species using the DC polarization test. In general, total ionic transference number (t_{ion}) and cationic (t_+)/anionic (t_-) transference numbers can be measured by performing DC polarization tests using appropriate electrodes. Electrodes which are blocking ions and permit electrons to move across under the effect of a DC potential are known as ion blocking electrodes. Using them, determining ion and electron contribution for conductivity can be done. Using anion blocking (or cation non-blocking) electrodes, cationic transference number, t_+ can be calculated. In DC polarization test, current variation with time across a SPE sandwiched between two electrodes is measured under the effect of a DC voltage.

A circular shaped sample was cut from the film with the optimized composition. It was sandwiched between two stainless steel (SS) electrodes and assembled in a spring-loaded sample

holder. A DC potential of 1 V was applied and the drop of current was measured as a function of time by using a computer controlled Metrohm Autolab Potentiostat M101. Another electrolyte film was sandwiched in between two identical Zn electrodes and assembled in a spring-loaded sample holder. Variation of the current with respect to time was measured under a DC potential of 0.1 V.

2.5 Determination of electrochemical stability window

Electrochemical stability window is a measure to indicate the safe potential window of a sample through which it has a resistance for reductive oxidative reactions. Accurate determination of electrochemical stability window of a SPE is a vital requirement from a practical point of view. It hints about a SPE to resist oxidative and reductive decomposition on electrodes.

Potential applied across a sample sandwiched in between two suitable electrodes is varied while measuring the current in order to determine the electrochemical stability window. This technique is known as linear sweep voltammetry (LSV) test. A constant current plateau in a linear sweep voltammogram that results from LSV test shows the endured potential range of an electrolyte.

In the present study, a SPE sample was assembled in between a SS electrode and a Zn electrode and loaded in side a sample holder sealed by an O ring. LSV test was done in the potential range 0.005 V-3.000 V at the scan rate of 10 mV s⁻¹ for the assembly of SS / SPE / Zn. In the three-electrode electrochemical setup, SS electrode served as the working electrode while Zn electrode was used as counter and reference electrodes. A computer controlled Metrohm Autolab Potentiostat M101 was used to obtain the current variation with potential.

2.6 Preparation of graphite electrodes

At room temperature, acetone and graphite were mixed in the ultrasonic homogenizer (Athena-Technology) to form a graphite paste. This paste was applied on the surfaces of two FTO glass plates which were cleaned and dried well before use. Surface area of the graphite electrode was 1 cm².

2.7 Fabrication of EDLCs

EDLCs were of the configuration, graphite/SPE/graphite. In terms of real world applications, there are some special performance indicators to be determined. Single electrode specific capacitance (C_{sc}) is of utmost importance since it indicates the storage capacity. In addition, its ability to withstand for continuous cycling is very useful in relation to long term applications. Insight into continuous charge discharge patterns is required to identify the rate of storing and dissipating charges. Three characterization tests namely electrochemical impedance spectroscopy (EIS) test, cyclic voltammetry (CV) test and galvanostatic charge discharge (GCD) test were carried out to investigate the performance of the EDLC fabricated under the present study.

2.8 Electrochemical impedance spectroscopy (EIS) test

EIS test for the fabricated EDLC was performed with the use of Metrohm Autolab Impedance Analyzer M101 at ambient temperature. Impedance data were gathered in the frequency range from 0.01 Hz-400 KHz.

2.9 Cyclic voltammetry (CV) test

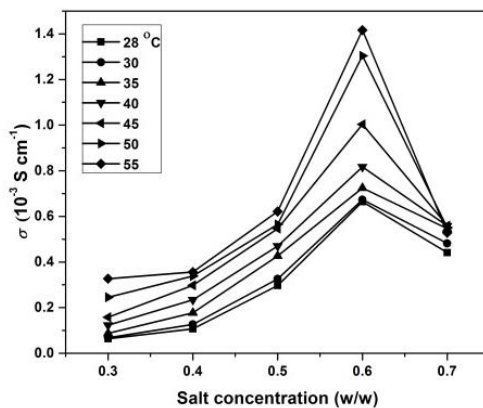


Fig. 1 Variation of conductivity of prepared SPEs with salt concentration at different temperatures

Potential window within which an EDLC is charged and discharged as well as the scan rate at which the EDLC is being cycled act as two determining factors of C_{sc} . Hence, by varying those, C_{sc} can be optimized. In addition, its durability for continuous operation can be assessed by continuously cycling under the corresponding potential window and the scan rate.

CV tests were done with the aid of a three electrode setup where one graphite electrode was used as the working electrode and the other electrode was used as counter and reference electrode. A computer controlled potentiostat module was used (Metrohm Autolab M101) to gather current and potential measurements. Continuous scanning was done for 1500 cycles.

2.10 Galvanostatic charge discharge (GCD) test

The ability of continuous functioning under a controlled current but within specific potential limits is also important for an EDLC to be employed for practical applications.

For GCD test, continuous charging and discharging was done under a constant current of $15 \mu\text{A}$ using a charge discharge unit (MTI Corporation, USA). Performance was observed for continuous 1000 cycles.

3. Results and discussion

3.1 Determination of the optimized composition of the electrolyte at different temperatures

The key role played by an electrolyte in any device is serving as the medium for ion conduction between the electrodes while assuring zero electronic conduction. Under this scenario, high ionic conductivity triggers the potential candidacy of an electrolyte for applications. Due to that, measuring as well as optimizing ionic conductivity is of pressing importance. The most widely accepted method to determine conductivity is via impedance measurements.

Conductivity, σ can be calculated with the equation given in Eq. (1).

$$\sigma = (1/R_b)t/A \quad (1)$$

where R_b is the bulk electrolyte resistance, t is the thickness and A is the area of cross section of SPE (Balamurugan and Ganesan 2020). R_b is sought via Nyquist plots drawn using impedance data.

Fig. 1 illustrates the conductivity variation at different temperatures for different salt concentrations of the SPEs prepared in the present study.

In general, σ is deeply integrated with mobility and concentration of ionic species according to the relationship

$$\sigma = ne\mu \quad (2)$$

where n , e and μ are the charge concentration, charge and mobility of charge species respectively. Hence, σ increases with increasing charge concentration as well as mobility. As per Fig. 1, σ has increased with temperature for all salt concentrations. Upon increasing temperature, charge species become thermally energized and as a result, their mobility rises. This improves σ of the samples. Another important feature in Fig. 1 is the presence of the maximum σ at the salt concentration of 0.6 ZnTF irrespective of temperature. The increasing and decreasing trend of σ before and after that concentration hints that there are some factors which govern the conductivity values with the salt concentration.

Fig. 2 illustrates a schematic diagram for the conductivity variation with the salt concentration.

As illustrated in Fig. 2, initial enhancement of conductivity with the salt concentration can be due to increase of mobile charge species population as reported by several studies (Kamisan *et al.* 2011). The reduction of σ upon further increase of salt concentration after 0.6 ZnTF may be due to formation of neutral ion clusters as well as decrease of mobility. A similar observation has been made for a MG49 NR based SPE. At high salt concentrations, the population of charge species is high and the mean distance among them is very short. This facilitates conducive environment for ion association leading to form neutral ion clusters. On the other hand, due to avalanche of charges, a noticeable reduction of mobility takes place. Both these factors lower the conductivity further (Ramesh *et al.* 2011, Ravindran and Vickraman 2012).

The optimum conductivity achieved at room temperature is $0.6 \times 10^{-3} \text{ S cm}^{-1}$. This is a desirable value from a practical point of view. A higher conductivity value ($7.55 \times 10^{-3} \text{ S cm}^{-1}$) has been reported for a SPE based on MG49 NR:0.7 M ammonium trifluoromethanesulfonate:propylene

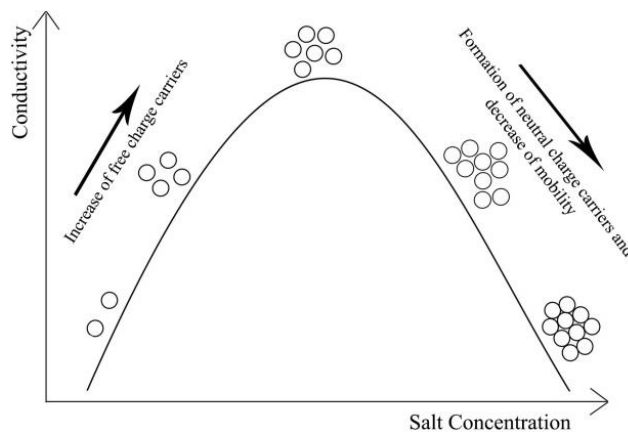


Fig. 2 Schematic representation illustrating the relationship between the salt concentration and the conductivity

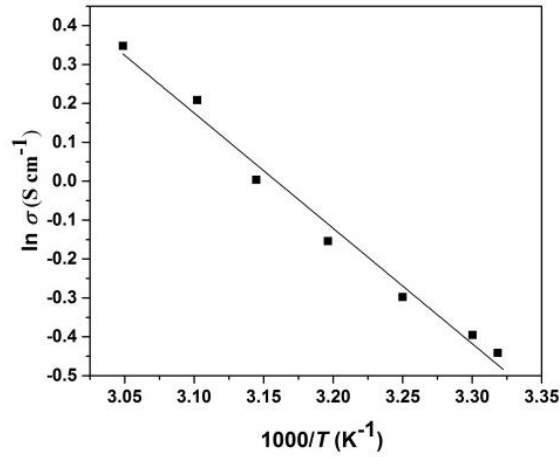


Fig. 3 Variation of $\ln \sigma$ with $1000/T$ for the optimized composition, MG49 NR:0.6 ZnTF of the SPE

carbonate:8% silicon dioxide (Kamisan *et al.* 2011). Conductivity of the present SPE is commendable compared to that system because the former contains a plasticizer as well as a nano filler which assist conductivity very much.

3.2 Conductivity mechanism

Ion conductivity mechanism of SPEs is usually explained as per the variation of conductivity with the temperature. Fig. 3 illustrates the plot of $\ln \sigma$ vs. $1000/T$ for the optimized SPE in this investigation.

Linear behavior of the graph confirms that the σ mechanism of the SPE obeys the Arrhenius model explained by Eq. (3)

$$\sigma = A \exp(E_a/k_B T) \quad (3)$$

Here, A is a pre-exponential factor, E_a is the activation energy, k_B is Boltzmann factor, T is the temperature.

When a conductivity behaviour of a system is due to jumping of ions into neighboring vacant sites, it follows Arrhenius behaviour (Zhang *et al.* 2017). Hence, the conductivity is assumed to be taken place via jumping of ions. That highly discloses the fact that ion mobility is a crucial requirement for satisfactory conductivity of the present system.

3.3 DC polarization test with ion blocking electrodes

Fig. 4 shows the DC polarization graph which exhibits the variation of current with time. As soon as the bias potential is applied, ions get polarized as they are blocked by SS electrodes. Due to that, a sudden drop of current occurs. A more or less constant current could be observed due to electrons. Here, it is to be noted that as a result of some reversible reactions, current due to electrons exhibit slight variations which are negotiable.

The total contribution of ions for conductivity which is defined as the ionic transference number, t_{ion} can be calculated using the Eq. (4).

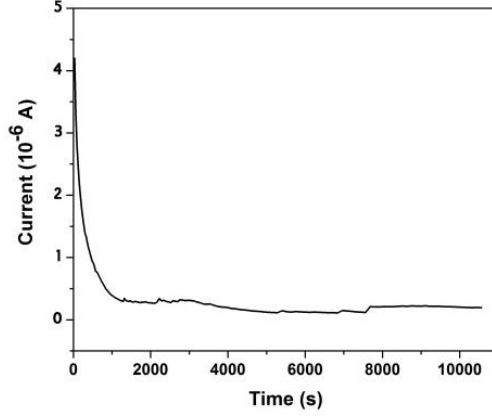


Fig. 4 DC polarization graph for the symmetric cell with SS electrodes under a DC bias potential of 1 V

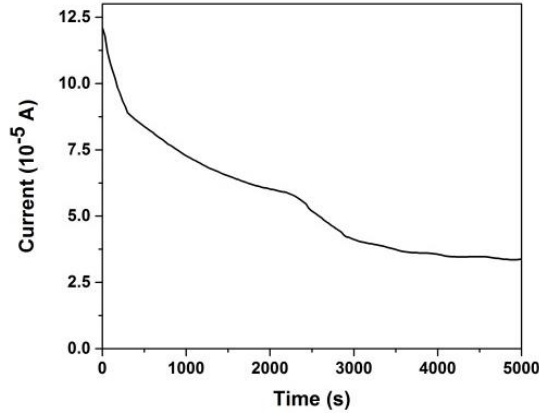


Fig. 5 DC polarization graph for the symmetric cell with Zn electrodes under a DC bias potential of 0.1 V

$$t_{ion} = (I_t - I_e)/I_t \quad (4)$$

where I_t is the total current due to ions and electrons and I_e is the current due to electrons. I_t and I_e were found to be 4.2×10^{-6} A and 0.21×10^{-6} A respectively.

According to the above equation, t_{ion} of the optimized sample was approximately 0.95. This predicts that overall conductivity of the SPE is predominantly ionic. In other words, this well proves the suitability of this SPE to be used as an electrolyte in devices due to dominant contribution of ions for conductivity. The electronic contribution is negligible. A near similar value has been reported for a SPE based on PEO, epoxidized NR and ammonium trifluoromethanesulfonate system (Khoon *et al.* 2016).

3.4 DC polarization test with cation non-blocking electrodes

Resulting DC polarization graph is shown in Fig. 5.

Cationic transference number, t_+ can be calculated using the Eq. (5)

$$t_+ = I_c/I_t \quad (5)$$

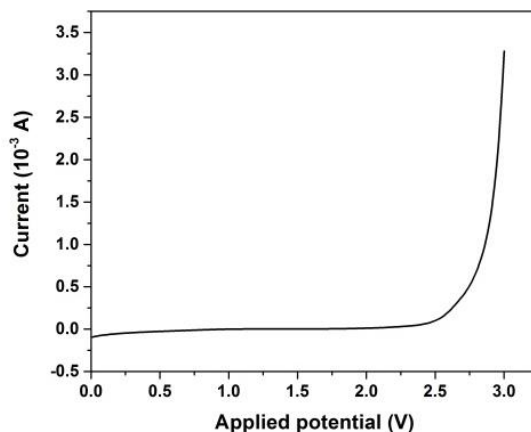


Fig. 6 Linear sweep voltammogram for the configuration, SS/SPE/Zn at the scan rate of 10 mV s⁻¹

where I_c and I_t are the steady state current due to cations and initial current due to both cations and anions respectively.

The value obtained for t_+ was 0.29 with I_c and I_t at 3.4×10^{-5} A and 11.62×10^{-5} A respectively. Contribution of cations on conductivity is seemed to be smaller than anions. This can be due to divalent nature of the cation, Zn.

3.5 Linear sweep voltammetry (LSV) test

Fig. 6 shows the linear sweep voltammogram for the cell with SS/SPE/Zn at the scan rate of 10 mVs⁻¹. It can be clearly seen here that the tolerable operating potential range of SPE is 0.25 V to 2.50 V where the current stays rather constant. The width of the stability window is about 2.25 V. This value of the working potential range appears to be sufficient enough to use in the EDLC. After 2.50 V, an abrupt increase of current exists. This can be due to decomposition of the electrolyte or the electrodes (Khoon *et al.* 2019, Ruschhaupt *et al.* 2020). An electrochemical stability window of 3.0 V has been reported by Khoon *et al* for a SPE based on polyvinylidene fluoride, MG49 NR and lithiumtrifluoromethaensulfonate. This is comparable to the obtained value in the present system as the latter contains a Li salt which inherently gives a wider stability window (Khoon *et al.* 2016).

3.6 Characterization of EDLC

3.6.1 Electrochemical Impedance Spectroscopy (EIS)

A typical Nyquist plot of an EDLC has a semi-circle at high frequency region denoting the bulk electrolyte resistance. Features at mid-range frequency region are being assigned to resistance for ion transport from the bulk electrolyte to the electrode interphase caused by non-uniform electrode pore size and electrode roughness (Yang *et al.* 2017). In the low frequency region, a spike appears as a result of the frequency dependence of ion diffusion at the electrolyte/electrode interface. This spike which should nearly parallel to the imaginary axis, reflects the capacitive nature (Fang and Binder 2006). Commonly, this spike appears as a tilted spike due to some factors like surface roughness of electrodes and problems at the interface.

Fig. 7 illustrates the Nyquist plot recorded for the graphite/ZnTF based SPE/graphite EDLC

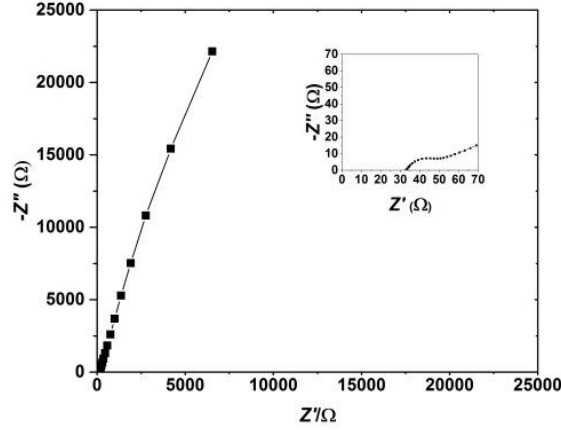


Fig. 7 Nyquist plot of the EDLC with ZnTF-MG49 NR based SPE and natural graphite electrodes

fabricated in this study. The insert highlights the high and mid frequency regions mainly. There is no semi-circle appearing in the high frequency region probably due to unavailability of required high frequency values for the measurements. Mid frequency semi-circular arc can be seen showcasing the electrode-electrolyte resistance. Absence of a complete semi-circle can be due to problems in the interface or the electrodes. However, the diameter of that arc which attributes to the charge transfer resistance (R_t) at the interface of the electrode and electrolyte is quiet small. This is beneficial for electrolyte ion diffusion and charge transfer. The spike at low frequency range is not perfectly vertical and that can be due to the surface roughness as well as non-uniform active layer thickness (Abdulhakeem *et al.* 2014).

AC impedance measurements can be used to investigate the capacitive properties of the EDLC further. The real part of the complex capacitance ($C'(\omega)$) and the imaginary part of the complex capacitance ($C''(\omega)$) are calculated based on the real ($Z'(\omega)$) and imaginary ($Z''(\omega)$) parts of the impedance using the Eqs. (6)-(7).

$$C'(\omega) = -Z''(\omega)/[\omega|Z(\omega)|^2] \quad (6)$$

$$C''(\omega) = Z'(\omega)/[\omega|Z(\omega)|^2] \quad (7)$$

where Z is the complex impedance (Tey *et al.* 2016).

By plotting graphs of $C'(\omega)$ and $C''(\omega)$ with frequency (Bode plots), single electrode specific capacitance, relaxation time and variation of capacitance with frequency can be determined.

Figs. 8(a) and 8(b) show the bode plots of $C'(\omega)$ and $C''(\omega)$ of the complex capacitance as a function of frequency.

C_{sc} obtained from Fig. 8(a) was 1.80 Fg^{-1} . There is a drastic drop of $C'(\omega)$ upon increasing frequency. It reaches close to zero with further increase of frequency. This well evidences the fact that capacitive properties become dominant at lower frequencies whereas resistive properties override capacitive properties with increase in frequency.

Relaxation time constant, τ_0 is a quantitative measure of reversible charge-discharge rate of the EDLC. It is hence the characteristic of the dynamic behavior of the EDLC (Kroupa *et al.* 2016). τ_0 can be calculated with the frequency f_0 , where maximum $C''(\omega)$ occurs (Fig. 8(b)) using the Eq. (8).

$$\tau_0 = 1/2\pi f_0 \quad (8)$$

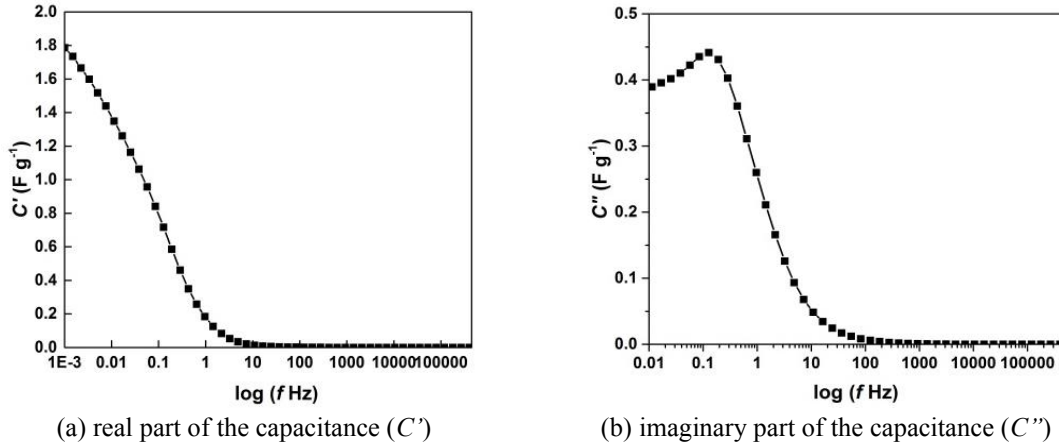
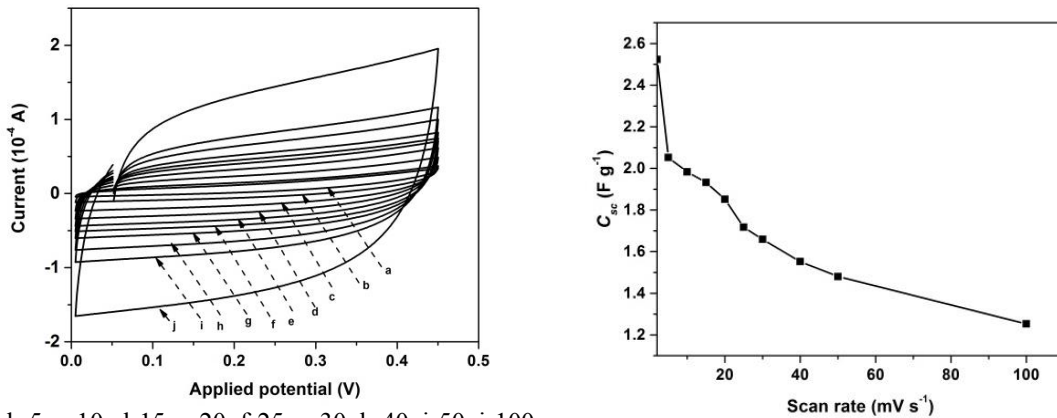


Fig. 8 Bode plots as a function of frequency (f) in logarithmic scale



a-2, b-5, c-10, d-15, e-20, f-25, g-30, h-40, i-50, j-100

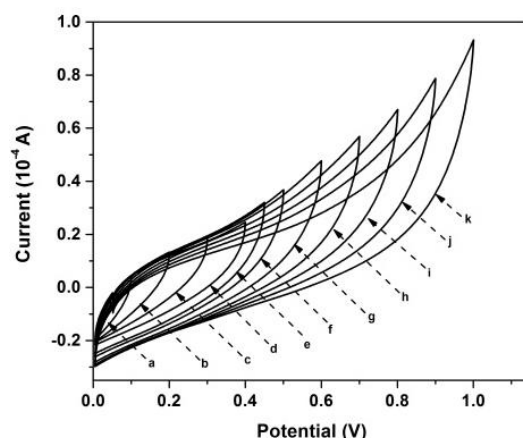
Fig 9(a) Cyclic voltammograms for this EDLC within the potential window of 0.005 to 0.45 V for different scan rates in mVs^{-1} Fig 9(b) Single electrode specific capacitance (C_{sc}) variation with respect to the scan rates

f_0 value obtained was 0.45 Hz. According to the equation, relaxation time constant is 0.35 s indicating fairly fast ion transfer. This is very much lower than the value reported for a gel polymer electrolyte based EDLC (Pal and Ghosh 2018). With that, it is noted that ion transfer is quite faster in the present NR based SPE.

3.6.2 Cyclic Voltammetry (CV) test

Figs. 9(a), 9(b) illustrate the cyclic voltammogrammes obtained for the fabricated EDLC at different scan rates and C_{sc} variation with different scan rates within the potential window, 0.005 to 0.45 V.

All cyclic voltammograms which have been obtained at different scan rates are having near mirror image symmetry for the current response about the zero current line. This result indicates the capacitive behavior and evidences the charge-discharge responses of the electric double layer are highly reversible (Fang and Binder 2006, Tey *et al.* 2016). Cyclic voltammograms of rectangular



a-0.1 b-0.2 c-0.3 d-0.4 e-0.45 f-0.5 g-0.6 h-0.7 i-0.8 j-0.9 k-1.0

Fig. 10 Cyclic voltammograms obtained at the scan rate of 10 mV s^{-1} within different potential windows (Minimum potential-0.005 V)

shape is one of the typical distinctive features of an EDLC. The resulting cyclic voltammograms show that characteristic with the almost rectangular shape. These carbon-based electrodes are not involved with the redox reactions and there is a rapid accumulation of charges at the electrode-electrolyte interface and within the electrode. This is evidenced with the absence of peaks in the curves (Yu *et al.* 2012). If redox reactions were present, peaks are appearing at potentials where such reactions occur.

C_{sc} can be calculated using the Eq. (9).

$$C_{sc} = 2(\int Idv) / mS\Delta S \quad (9)$$

where $\int Idv$ is the area under cyclic voltammograms, m is the mass of an electrode. S and ΔV are the scan rate and width of the potential window respectively (Kroupa *et al.* 2016).

Value of C_{sc} decreased with the increasing scan rate. This indicates the fact that reactions leading to charge storage in EDLC are highly dependent on the scan rate (Arslan *et al.*). At slow scan rates, there is an ample time to complete the reactions. In addition to that, charges have adequate time to travel through the pores of electrode materials at slow scan rates. These all contribute for higher C_{sc} . In contrast, reactions may not be completed at the high scan rates (Romanitan *et al.* 2018, Pandey and Rastogi 2012). As a result low C_{sc} values are present at high scan rates. Similar observations have been made by Pal *et al.* and Das *et al.* for EDLCs fabricated with ionic liquid based electrolytes (Pal and Ghosh 2018, Das and Ghosh 2017). They suggest that loss of energy increases at high scan rates lowering the charge stored on the surface electrode and ultimately resulting decrease of C_{sc} . The scan rate of 10 mV s^{-1} was chosen as the suitable scan rate for further investigations.

For proper charge storage mechanism, presence of the required potential window is also very important. However, a higher potential window than the electrochemical stability window destroys the EDLC. It is due to decomposition of electrodes and/or electrolyte itself (Kroupa *et al.* 2016). Hence, selection of the most suitable potential window is very essential to get the proper charge storage function.

The cyclic voltammograms obtained for the different potential windows and at the scan rate of 10 mV s^{-1} are illustrated in Fig. 11.

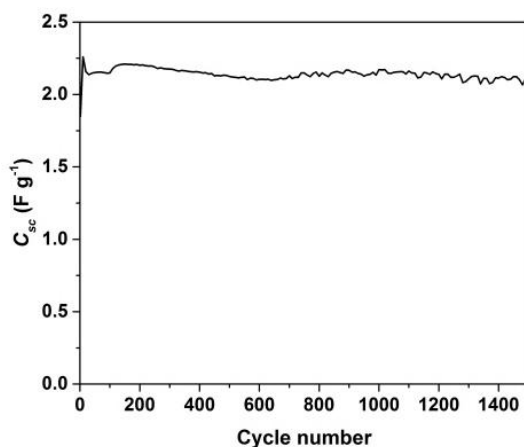


Fig. 11 Variation of single electrode specific capacitance of the EDLC as a function of cycle number at the scan rate of 10 mV s^{-1}

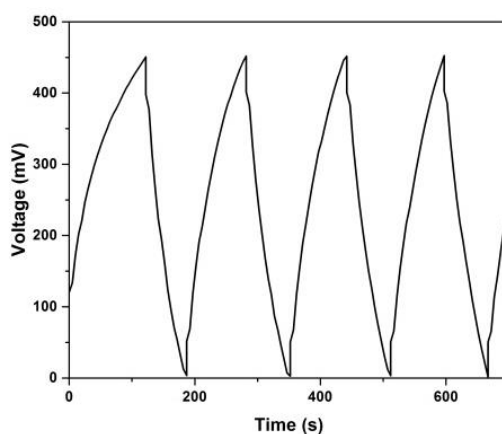


Fig. 12 Initial charge discharge curves obtained under constant current of $15 \mu\text{A}$

Peaks are not seen in all windows due to lack of redox reactions in the EDLC. When the width of the potential window was increased beyond the 0.45 V, the shape started to distort. This can be due to undesirable reactions which might cause the degradation of EDLC. Therefore, 0.005-0.450 V was selected as the optimized potential window for further cycling (Kroupa *et al.* 2016, Lu *et al.* 2006).

Fig. 12 illustrates C_{sc} variation for 1500 continuous cycles.

The potential window was 0.005-0.45 V and the scan rate was 10 mVs^{-1} . Initial C_{sc} of the EDLC was about 2.26 F g^{-1} . It decreased with the cycle number and after 1500 cycles, C_{sc} was about 2.10 F g^{-1} . This can be occurred due to loss of interfacial contacts between the electrode and electrolyte and also due to degradation of electrolyte and or electrodes. But, the rate of reduction of C_{sd} was rather low which is a good sign for practical applications.

3.6.3 Galvanostatic Charge Discharge test

Galvanostatic charge discharge (GCD) test of an EDLC allows tracing some important features

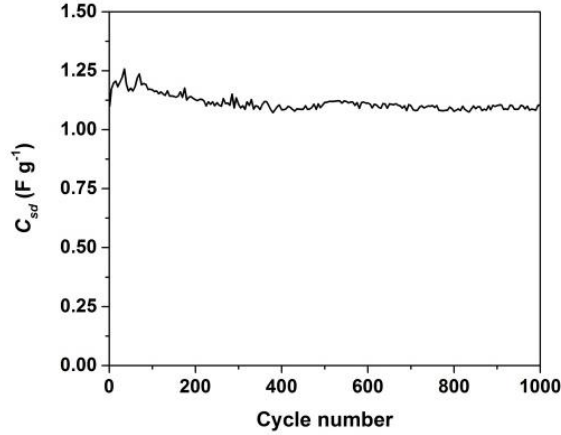


Fig. 13 Single electrode specific discharge capacitance (C_{sd}) variation for 1000 cycles for the EDLC

such as the reversibility of the device, capacitive nature and presence of any decomposition reactions. Fig. 13 exhibits the initial charge discharge curves obtained under the GCD test. Discharge behavior is linear as observed by Das *et al* for an EDLC based on an ionic liquid electrolyte (Arslan and Hur 2021). This evidences the presence of non-faradic capacitive charge storage mechanism. Theoretically, shapes of the charge discharge cycles indicate the reversibility of the device. Triangular shapes are normally present for EDLCs and equilateral triangle shapes symbolize good reversibility during charge/discharge cycles. However, the resulted charge discharge shapes are having triangular shape to some extent but they are not perfect equilateral triangles. This implies the presence of some issues with reversibility. Due to possible problems in the structure of SPE as well as the graphite electrodes, unique ion movement may not take place. As a result, reversibility problems may arise. This observation is further confirmed with the non-equal charge discharge times at each cycle. Generally, charge discharge time periods should be equal for each cycle if there is a good reversibility. Investigating the continuous cycling ability of any electrochemical device is extremely important from a practical point of view. It assists to obtain a guarantee about the active life time.

There is a distinct potential drop about 50 mV at the beginning of each discharge process. This drop is ascribed to the internal resistance of the electrodes accompanied with resistance in electrical connection and the resistance due to the migration of ions in electrodes.

The single electrode specific discharge capacitance (C_{sd}) was calculated using the Eq. (10).

$$C_{sd} = I\Delta t/m\Delta V \quad (10)$$

where I is the constant current, m is the mass of the single electrode and $\Delta V/\Delta t$ is the rate of drop of potential excluding IR drop during discharge (Fletcher *et al.* 2014).

Fig. 14 presents the variation of C_{sd} for 1000 cycles. Initially, a slight increase of C_{sd} could be observed. Soon after fabrication, EDLC does not have well formed interfaces. Upon initiation of cycling, it can attain maturity and due to that, an initial increase of C_{sd} can arise. However, further cycling has caused a reduction of C_{sd} followed by a constant state. While charging and discharging the EDLC continuously, some decomposition may take place lowering C_{sd} . With time, a passivation layer may be formed resulting a constant C_{sd} . Pandey *et al* have reported a fast initial decrease of C_{sd} for an EDLC based on activated charcoal electrodes (Pandey *et al* 2012). According to them,

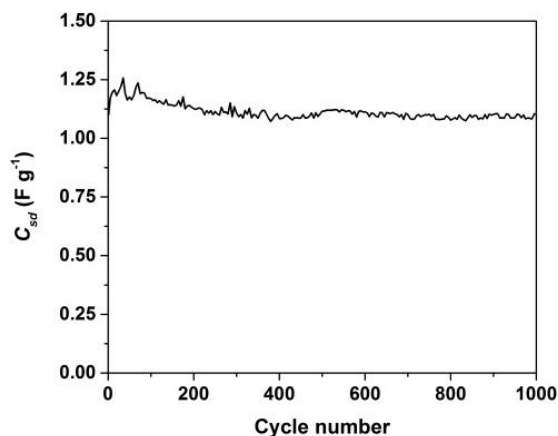


Fig. 14 Single electrode specific discharge capacitance (C_{sd}) variation for 1000 cycles for the EDLC

that is due to either consumption of some charges for irreversible reactions or filling of micro-pores of electrodes during charging. Absence of fast reduction of C_{sd} in the present study reveals the absence of such irreversible reactions as well as filling of any pores in the electrodes. For the first cycle, C_{sd} was 1.17 F g^{-1} . After 1000 cycles, it was found to be 1.10 F g^{-1} and hence, the reduction was 5.9 % which is quite small.

4. Conclusions

NR based SPE was prepared with 49% methyl grafted natural rubber (MG49) and zinc trifluoromethanesulfonate (ZnTF). Different compositions of electrolytes were prepared using the solvent casting technique. The highest room temperature conductivity of $0.6 \times 10^{-3} \text{ S cm}^{-1}$ was obtained with the composition NR:0.6 ZnTF (by weight basis). The resulting electrolyte film was a mechanically stable, free standing film. Variation of conductivity with temperature follows Arrhenius behavior suggesting ion conduction takes place via hopping mechanism. Type of charge which contributes for conductivity was traced by DC polarization test. Sample was predominantly an ionic conductor. Electrochemical stability window of the SPE was about 2.495 V according to LSV test.

The EDLC with configuration NG/NR-ZnTF based SPE/NG was fabricated successfully at room temperature. Capacitive features are dominant at low frequency range. Continuous CV test was done between the optimized potentials of 0.005 V and 0.45 V at a scan rate of 10 mV s^{-1} . C_{sc} of the EDLC was about 2.26 F g^{-1} . The initial C_{sd} at the first cycle was found to be 1.17 F g^{-1} . After about 1000 charge discharge cycles, the value reduced down to 1.10 F g^{-1} . A low reduction of C_{sd} assures the suitability of the fabricated EDLC for long term applications.

Acknowledgement

The research described in this paper was financially supported by the National Research Council Sri Lanka under the research grant NRC 17-006. Also, Associated Speciality Rubbers (PVT) Ltd,

Kegalle, Sri Lanka and Bogala Graphite Lanka, Bogala, Sri Lanka are highly acknowledged for providing samples.

References

- Abdulkhakeem, B., Farshad, B., Damilola, M., Fatemeh, T., Mopeli, F., Julien, D. and Ncholu, M. (2014), "Morphological characterization and impedance spectroscopy study of porous 3D carbons based on graphene foam-PVA/phenol-formaldehyde resin composite as an electrode material for super capacitors", *RSC Adv.*, **4**(73), 39066-39072. <https://doi.org/10.1039/C4RA05425C>.
- Abruña, H.D., Kiya, Y. and Henderson, J.C. (2008), "Batteries and electrochemical capacitors", *Phys. Today*, **61**(12), 43-47. <https://doi.org/10.1063/1.3047681>.
- Arslan, A. and Hur, E. (2012), "Super capacitor applications of polyaniline and poly(N-methylaniline) coated pencil graphite electrode", *Int. J. Electrochem. Sci.*, **7**, 12558-12572.
- Aziz, A.F., Nazir, K., Ayub, S.F., Adam, N.I., Yahya, M.Z. and Ali, A.B.M.M. (2018), "Electrochemical properties of polymer electrolytes treated with 6ppd on 30% poly(methyl methacrylate) grafted natural rubber", *Malay. J. Anal. Sci.*, **22**(3), 491-498. <https://doi.org/10.17576/mjas-2018-2203-17>.
- Balamurugan, S. and Ganesan, S. (2020), "Novel cobalt redox materials admitted in natrosol polymer with a thiophene based additive as a gel polymer electrolyte to tune up the efficiency of dye sensitized solar cells", *Electrochim. Acta*, **329**, 135169. <https://doi.org/10.1016/j.electacta.2019.135169>.
- Chandra, A. (2013), "Synthesis and dielectric studies on PEO-PVP blended solid polymer electrolytes", *Ind. J. Pure Appl. Phys.*, **51**, 788-791.
- Das, S. and Ghosh, A. (2017), "Solid polymer electrolyte based on PVdF-HFP and ionic liquid embedded with TiO₂ nanoparticle for electric double layer capacitor (EDLC) application", *J. Electrochem. Soc.*, **164**, F1348-F1353.
- Fang, B. and Binder, L. (2006), "A modified activated carbon aerogel for high-energy storage in electric double layers", *J. Power Sour.*, **163**, 616-622. <https://doi.org/10.1016/j.jpowsour.2006.09.014>.
- Fletcher, S., Black, V.J. and Kirkpatrick, I. (2014), "A universal equivalent circuit for carbon based super capacitors", *J. Solid State Electrochem.*, **18**, 1377-1387. <https://doi.org/10.1007/s10008-013-2328-4>.
- Glasse, M.D., Idris, R., Latham, R.J., Linford, R.G. and Schlindwein, W.S. (2002), "Polymer electrolytes based on modified natural rubber", *Solid State Ionics*, **147**, 289-294.
- Idris, R., Glasse, M.D., Latham, R.J., Linford, R.G. and Schlindwein, W.S. (2001), "Polymer electrolytes based on modified natural rubber for use in rechargeable lithium batteries", *J. Power Sour.*, **94**, 206-211.
- Kamisan, A.S., Kudin, T.I.T., Ali, A.M.M. and Yahya, M.Z.A. (2011), "Polymer gel electrolytes based on 49% methyl grafted natural rubber", *Sains Malaysiana*, **40**, 49-54.
- Kamisan, A.S., Kudin, T.I.T., Ali, A.M.M. and Yahya, M.Z.A. (2011), "Electrical and physical studies on 49% methyl grafted natural rubber based composite polymer gel electrolytes", *Electrochim. Acta*, **57**, 207-211. <https://doi.org/10.1016/j.electacta.2011.06.096>.
- Khoon, L.T., Ataollahi, N., Hassan, N.H. and Ahmad, A. (2016), "Studies of porous solid polymeric electrolytes based on poly(vinylidene fluoride) and poly(methyl methacrylate) grafted natural rubber for applications in electrochemical devices", *J. Solid State Electrochem.*, **20**(1), 203-213. <https://doi.org/10.1007/s10008-015-3017-2>.
- Khoon, L.T., Zaini, N.F.M., Mobarak, N.N., Hassan, N.H., Noor, S.A.M., Mamat, S., Loh, K.S., KuBulat, K.H., Su'ait, M.S. and Ahmad, A. (2019), "PEO based polymer electrolyte comprised of epoxidized natural rubber material (ENR50) for Li ion polymer battery application", *Electrochim. Acta*, **316**, 283-291. <https://doi.org/10.1016/j.electacta.2019.05.143>.
- Kroupa, M., Offer, G.J. and Kosek, J. (2016), "Modelling of supercapacitors: Factors influencing performance", *J. Electrochem. Soc.*, **163**(10), A2475-A2487. <https://doi.org/10.1149/2.0081613jes>.
- Libich, J., Maca, J., Vondrak, J., Cech, O. and Sedlarikova, M. (2018), "Supercapacitors: Properties and applications", *J. Energy Storage*, **17**, 224-227. <https://doi.org/10.1016/j.est.2018.03.012>.
- Lu, W., Henry, K., Turchi, C. and Pellegrino, J. (2006), "Incorporating ionic liquid gel electrolytes into

- polymer gels for solid-state ultra capacitors”, *J. Electrochem. Soc.*, **155**(5), A361-A367. <https://doi.org/10.1149/1.2869202>.
- Mohamed, S.N., Johari, N.A., Ali, A.M.M., Harun, M.K. and Yahya, M.Z.A. (2008), “Electrochemical studies on epoxidised natural rubber based polymer electrolytes for lithium air cells”, *J. Power Sour.*, **183**, 351-354. <https://doi.org/10.1016/j.jpowsour.2008.04.048>.
- Nimah, Y. L., Cheng, M.Y., Cheng, J.H., Rick, J. and Hwang, B.J. (2015), “Solid state polymer nanocomposite electrolyte of TiO₂/PEO/NaClO₄ for sodium ion batteries”, *J. Power Sour.*, **278**, 375-381. <https://doi.org/10.1016/j.jpowsour.2014.11.047>.
- Pal, P. and Ghosh, A. (2018), “Highly efficient gel polymer electrolytes for all solid state electrochemical charge storage devices”, *Electrochim. Acta*, **278**, 137-148. <https://doi.org/10.1016/j.electacta.2018.05.025>.
- Pandey, G.P. and Rastogi, A.C. (2012), “Solid-state super capacitors based on pulse polymerized poly(3,4-ethylenedioxythiophene) electrodes and ionic liquid gel polymer electrolyte”, *J. Electrochem. Soc.*, **159**(10), A1664-A1671. <https://doi.org/10.1149/2.047210jes>.
- Pandey, G.P., Hashmi, S.A. and Kumar, Y. (2010), “Performance studies of activated charcoal based electrical double layer capacitors with ionic liquid gel polymer electrolytes”, *Energy Fuel.*, **24**, 6644-6652. <https://doi.org/10.1021/ef1010447>.
- Pandey, G.P., Kumar, Y. and Hashmi, S. (2010), “Ionic liquid incorporated polymer electrolytes for super capacitor application”, *Ind. J. Chem.*, **49A**, 743-751.
- Ramesh, S., Liew, C.W. and Ramesh, K. (2011), “Evaluation and investigation on the effect of ionic liquid onto PMMA-PVC gel polymer blend electrolytes”, *J. Non-Cryst Solid.*, **357**, 2132-2138. <https://doi.org/10.1016/j.jnoncrysol.2011.03.004>.
- Ravindran, D. and Vickraman, P. (2012), “Mg²⁺ ionic conductivity behavior of mixed salt system in PVA-PEG blend matrix”, *Int. J. Scientif. Res. Publ.*, **2**(12), 1-4.
- Romanitan, C., Varasteanu, P., Mihalache, I., Culita, D., Somacescu, S., Pascu, R. and Kusko, M. (2018), “High-performance solid state super capacitors assembling graphene interconnected networks in porous silicon electrode by electrochemical methods using 2,6-dihydroxynaphthalen”, *Scientif. Report.*, **8**(1), 9654-9668. <https://doi.org/10.1038/s41598-018-28049-x>.
- Ruschhaupt, P., Pohimann, S., Varzi, A. and Passerini, S. (2020), “Determining realistic electrochemical stability window of electrolytes for EDLC”, *Batter. Super Capacit.*, **3**, 1-11. <https://doi.org/10.1002/batt.202000009>.
- Salleh, N.S., Aziz, S.B., Aspanut, Z. and Kadir, M.F.Z. (2016), “Electrical impedance and conduction mechanism analysis of biopolymer electrolytes based on methyl cellulose doped with ammonium iodide”, *Ionics*, **22**, 2157-2167. <http://doi.org/10.1007/s11581-016-1731-0>.
- Silakul, P. and Magaraphan, R. (2013), “Gel Polymer Electrolyte from Poly(Acrylamide) coated on natural rubber latex by topology-controlled emulsion polymerization for dye sensitized solar cells application”, *Adv. Mater. Res.*, **747**, 325-328. <https://doi.org/10.4028/www.scientific.net/AMR.747.325>
- Simon, P. and Gogotsi, Y. (2008), “Materials for electrochemical capacitors”, *Nat. Mater.*, **7**(11), 845-854. <https://doi.org/10.1038/nmat2297>.
- Tey, J.P., Careem, M.A., Yarmo, M.A. and Arof, A.K. (2016), “Durian shell-based activated carbon electrode for EDLCs”, *Ionics*, **22**(7), 1209-1216. <https://doi.org/10.1007/s11581-016-1640-2>.
- Yang, I., Kim, S.G., Kwon, S.H., Kim, M.S. and Jung, J.C. (2017), “Relationships between pore size and charge transfer resistance of carbon aerogels for organic electric double-layer capacitor electrodes”, *Electrochim. Acta*, **223**, 21-30. <https://doi.org/10.1016/j.electacta.2016.11.177>.
- Yu, H., Wu, J., Fan, L., Lin, Y., Xu, K., Tang, Z., Cheng, C., Tang, S., Lin, J. and Huang, M. (2012), “A novel redox-mediated gel polymer electrolyte for high-performance super capacitor”, *J. Power Sour.*, **198**, 402-407. <https://doi.org/10.1016/j.jpowsour.2011.09.110>.
- Zhang, Q., Liu, K., Ding, F. and Liu, X. (2017), “Recent advances in solid polymer electrolytes for lithium batteries”, *Nano Res.*, **10**(12), 4139-4174. <https://doi.org/10.1007/s12274-017-1763-4>.